Kow, Y. W., & Wallace, S. S. (1985) *Proc. Natl. Acad. Sci. U.S.A. 82*, 8354–8358.
Kow, Y. W., & Wallace, S. S. (1987) *Biochemistry 26*, 8200–8206.
Kow, Y. W., Ide, H., & Wallace, S. S. (1987) in *Anticarcinogenesis and Radiation Protection* (Cerutti, P. A., Nygaard, O. F., & Simic, M. G., Eds.) pp 135–138, Plenum Press, New York and London.
Kowalski, D. (1979) *Anal. Biochem. 93*, 346–354.
Kunkel, T. A., Schaaper, R. M., & Loeb, L. A. (1983) *Biochemistry 22*, 2378–2384.
Lindahl, T., & Nyberg, B. (1972) *Biochemistry 11*, 3610–3618.
Lindahl, T., Ljungquist, S., Siegert, W., Nyberg, B., & Sperens, B. (1977) *J. Biol. Chem. 252*, 3286–3294.
Liuzzi, M., & Talpaert-Borlē, M. (1985) *J. Biol. Chem. 260*, 5252–5258.
Liuzzi, M., Weinfeld, M., & Paterson, M. C. (1987) *Biochemistry 26*, 3315–3321.
Loeb, L. A., & Preston, B. D. (1980) *Annu. Rev. Genet. 20*, 201–230.
Londesborough, J. (1980) *Eur. J. Biochem. 105*, 211–215.
Maniatis, F., Fritsch, E. F., & Sambrook, J. (1982) in *Molecular Cloning: A Laboratory Manual*, Cold Spring Harbor Laboratory Press, Cold Spring Harbor, NY.
Melamede, R. J., Kow, Y. W., & Wallace, S. S. (1987) in *Anticarcinogenesis and Radiation Protection* (Cerutti, P. A., Nygaard, O. F., & Simic, M. G., Eds.) pp 139–144, Plenum Press, New York and London.
Mosbaugh, D. W., & Linn, S. (1980) *J. Biol. Chem. 255*, 11743–11752.
Niwa, O., & Moses, R. E. (1981) *Biochemistry 20*, 238–344.
Paek, K. H., & Walker, G. C. (1986) *J. Bacteriol. 165*, 763–770.
Povirk, L., & Goldberg, I. H. (1985) *Proc. Natl. Acad. Sci. U.S.A. 82*, 3182–3186.
Richardson, C. C., & Kornberg, A. (1964) *J. Biol. Chem. 239*, 242–250.
Royer-Pokora, B., Gordon, L. K., & Haseltine, W. A. (1981) *Nucleic Acids Res. 9*, 4594–4609.
Sammartano, L. J., & Tuveson, R. W. (1983) *J. Bacteriol. 156*, 904–906.
Sagher, D., & Strauss, B. (1983) *Nucleic Acids Res. 13*, 4285–4298.
Seeberg, H., & Steinum, A. (1980) *J. Bacteriol. 141*, 1424–1427.
Talpaert-Borlē, M. (1987) *Mutat. Res. 181*, 45–56.
Talpaert-Borlē, M., & Liuzzi, M. (1983) *Biochim. Biophys. Acta 740*, 410–416.
Taylor, A. F., & Weiss, B. (1982) *J. Bacteriol. 151*, 351–357.
Teoule, R. (1987) *Int. J. Radiat. Biol. 51*, 573–589.
Thomas, K. R., & Olivera, B. M. (1978) *J. Biol. Chem. 253*, 424–429.
Warner, H. R., Demple, B., Deutsch, W. D., Kane, C. M., & Linn, S. (1980) *Proc. Natl. Acad. Sci. U.S.A. 77*, 4602–4606.
Weiss, B. (1976) *J. Biol. Chem. 251*, 1896–1901.
Weiss, B. (1981) *Enzymes (3rd Ed.) 14*, 203–231.
Weiss, B., & Grossman, L. (1987) *Adv. Enzymol. Relat. Areas Mol. Biol. 60*, 1–34.
Wu, R., Ruben, G., Siegel, B., Jay, E., Spielman, P., & Tu, C. D. (1976) *Biochemistry 15*, 734–740.
Yajko, D. M., & Weiss, B. (1975) *Proc. Natl. Acad. Sci. U.S.A. 72*, 688–692.

The Location of DNA in Complexes of recA Protein with Double-Stranded DNA. A Neutron Scattering Study†

Elisabeth DiCapua,‡ Manfred Schnarr,§ and Peter A. Timmins*,‡
Institut Laue-Langevin, 156X, 38042 Grenoble Cedex, France, and Institut de Biologie Moléculaire et Cellulaire, 15, rue Descartes, 67000 Strasbourg, France

Received July 7, 1988; Revised Manuscript Received November 29, 1988

ABSTRACT: Purified recA protein is found as rodlike homopolymers, and it forms filamentous complexes with double-stranded DNA that are stable in the presence of ATPγS, a nonhydrolyzable analogue of ATP. The structure of these filaments has been described in some detail by electron microscopy. Here we confirm the mass per length of 6.5 recA/100 Å in solution by small-angle neutron scattering and extend the analysis to homopolymers of recA protein, finding a mass per length of about 7 recA/100 Å and a radial mass distribution (cross-sectional radius of gyration) significantly different for the two filaments. The models proposed so far for the structure of the complex have placed the DNA in the center of the filament. Here we verify this assumption using small-angle neutron scattering to locate the DNA in the complexes, exploiting the contrast variation method in D_2O/H_2O mixtures. Model calculations show that the natural contrast difference between DNA and protein is not sufficient to locate the DNA (which accounts for only 4.7% of the mass in the complex). When deuterated DNA is used, the contrast difference is enhanced, and model calculations and experiment then converge, indicating that the DNA is indeed near the axis of the complex.

Homologous recombination in *Escherichia coli* is dependent on the *recA* gene product. In vitro, the purified protein is able to perform strand exchange. This reaction was found to be initiated by the covering of one of the DNA partners to form a filamentous structure, the presynaptic complex, which will subsequently interact with the second DNA molecule [reviewed in Howard-Flanders et al. (1984)].

The presynaptic complex is formed in the presence of ATP on single-stranded DNA (Flory et al., 1984); it is known to

† This project was supported by the European Molecular Biology Organization (long-term fellowship to E.D.C.).
‡ Institut Laue-Langevin.
§ Institut de Biologie Moléculaire et Cellulaire.

0006-2960/89/0428-3287$01.50/0

grow into adjacent double-stranded regions (Cassuto & Howard-Flanders, 1986), but we do not know whether these regions can act as presynaptic complex. Reciprocal strand exchange between two double strands can occur when initiated at a single-stranded gap (West et al., 1981). In any case, the complex with double-stranded DNA is a substrate for branch migration, the reaction subsequent to synapsis at the contact site.

The three-dimensional structure of the presynaptic complex will give clues as to the mechanism of the interesting reaction of strand exchange. The complex can be stabilized with ATPγS,[1] a nonhydrolyzable analogue of ATP (West et al., 1980). Electron microscopy has revealed identical outer appearance of the complexes with single-stranded and double-stranded DNA (DiCapua et al., 1982; Koller et al., 1983). Image reconstruction shows 6.2 recA subunits per turn of a helical protein coat of 95-Å pitch and about 100-Å diameter (Egelman & Stasiak, 1986). The inner details have however escaped structural analysis. Indirect methods, biochemistry and DNA topology, reveal clear parameters for double-stranded DNA in the complex: the DNA is stretched by a factor of 1.5 (Stasiak et al., 1981), and its helicity is reduced from 10.5 to 18.5 base pairs per turn (Stasiak & DiCapua, 1983). The stoichiometry is 1 recA per 3 base pairs (DiCapua et al., 1982; Dombroski et al., 1983), and recA protects the DNA from methylation by dimethyl sulfate in its minor groove (DiCapua & Müller, 1987). On the other hand, the same analysis with single-stranded DNA complexes leads to much less defined results: the stoichiometry varies with conditions between 3 and 8 nucleotides per recA, the contour length of the DNA accordingly does not acquire a unique value [reviewed in DiCapua and Koller (1987)], and the protection from chemical modification is less regular; the single-stranded DNA is in fact quite accessible to dimethyl sulfate (Leahy & Radding, 1986) while however completely protected from DNases (DiCapua, unpublished results; Bryant et al., 1985).

Neutron scattering, exploiting the contrast variation method in D_2O/H_2O mixtures [reviewed in Timmins and Zaccai (1988)], allows another approach to localize the DNA in the complex. Its power is unique in being able to distinguish protein and DNA owing to their different chemical compositions, leading to different scattering density for neutrons. The limitation in our case is the small amount of DNA present in the complex (4.7% by weight for the double-stranded DNA complex, less for the single strand). We thus had to limit the study to the double strand. This paper describes our approach and our experimental localization of the DNA in the center of the complex. Mass per unit length and cross-sectional dimensions are also obtained from the analysis.

Materials and Methods

Materials

RecA protein (M_r = 37.8K) was extracted from strain pDR 1453/KM 4104 according to Weinstock et al. (1979). The purity after a phosphocellulose column was considered sufficient: the A_{280}/A_{260} ratio was between 1.6 and 1.7 (Craig & Roberts, 1981), suggesting no major contaminant; no change in this ratio nor in specific ATPase activity could be obtained by either DEAE-cellulose, Sephacryl 300, or single-stranded DNA–cellulose chromatography, suggesting that what may be won in chemical purity is concomitantly lost in inactivation of the product. Heavily overloaded, Coomassie-stained SDS–acrylamide gels reveal contaminating bands, none of which exceeded 1% of the main band intensity upon scanning on a Shimadzu CS 930; evaluation of the recA band at a peak threshold of 0.5% (of the main band) led to a figure of 82% recA. As staining of gels is not quantitative over a broad range of concentrations nor between different protein species, this value is at best indicative. The presence of these contaminants leads to an overestimation of the concentration, which was determined by using an extinction coefficient $E^{1\%}_{277nm}$ of 6.33 (Tsang et al., 1985). Using $E^{1\%}_{280nm}$ = 5.9 (Craig & Roberts, 1981) increases the value by 5%.

DNA. Deuterated DNA was obtained from *E. coli* grown in synthetic medium (Kalbitzer et al., 1985). *Calf thymus DNA* was from Sigma. *pUC8 plasmid DNA* was extracted by a cleared lysate. All DNAs were repurified by protease and RNase treatment, phenol extraction, and ethanol and 2-propanol precipitations.

Stable complexes were formed at 4 mg/mL recA protein and 0.28 mg/mL DNA (25% excess DNA relative to a stoichiometry of 1 recA per 3 base pairs) in a buffer containing 20 mM potassium phosphate, pH 6.8, 5% glycerol, 2 mM magnesium acetate, and 0.5 mM ATPγS (Boehringer), by incubation at 37 °C for 30 min. Complex formation was verified by finding the expected amount of the DNA protected from DNases [DNase I (Boehringer grade II) and phosphodiesterase I (Sigma)]. The homopolymer of recA was formed under the same conditions except that the DNA was omitted.

Methods

Small-Angle Neutron Scattering (SANS). SANS data were collected on the instrument D11 (Ibel, 1976) at the Institut Laue-Langevin, Grenoble. The two-dimensional multidetector was placed at a distance of 5 m from the sample, and incident neutrons of wavelength λ = 10 Å were selected by means of a helical slot velocity selector ($\Delta\lambda/\lambda$ = 8%). Samples were contained in quartz cuvettes (Hellma, Paris, France) of pathlength 1 or 2 mm and thermostated at 15 ± 1 °C.

Data Analysis. Scattering patterns were radially averaged and corrected for buffer scattering and detector response by using standard programs (Ghosh, 1981). The scattering from a 1 mm thick sample of water is used for correction of the differential response of the detector and also allows the data to be placed on an absolute scale (Jacrot & Zaccai, 1981).

The corrected scattering curves $I(Q)$ versus Q [$Q = (4\pi \times \sin\theta)/\lambda$, 2θ = scattering angle, λ = neutron wavelength] were interpreted via the Guinier approximation for rodlike particles:

$$I(Q)Q = [I(Q)Q]_{Q\to 0} \exp(-R_c^2Q^2/2)$$

Hence a plot of ln $I(Q)Q$ versus Q^2 yields two independent parameters, the cross-sectional radius of gyration R_c and the extrapolated zero-angle scattering $[I(Q)Q]_{Q\to 0}$.

R_c is related to the radial distribution of scattering density and for a homogeneous distribution is equal to $1/\sqrt{2}$ times the cross-sectional radius.

$[I(Q)Q]_{Q\to 0}$, when calculated on an absolute scale, reflects the excess scattering mass and is related to the mass per unit length (μ) by the expression (Torbet et al., 1981)

$$\frac{[I(Q)Q]_{Q\to 0}}{C} = \pi A N_A \mu \left[\frac{\sum b}{M_r} - \rho_s\left(\frac{V}{M_r}\right)\right]^2$$

where $[I(Q)Q]_{Q\to 0}$ is as defined above and is normalized to the scattering of a 1 mm thick sample of water under the same geometric conditions, C = sample concentration in g/L, and

[1] Abbreviations: SANS, small-angle neutron scattering; R_c, cross-sectional radius of gyration; ATPγS, adenosine 5′-*O*-(3-thiotriphosphate); ds DNA, double-stranded DNA; H-DNA, hydrogenated DNA; D-DNA, deuterated DNA.

N_A = Avogadro's number. A is an experimental term that includes geometrical and neutron beam parameters:

$$A = \frac{4\pi T_s t}{1 - T_w}$$

where t = cell thickness in cm, T_s = neutron transmission of sample, and T_w = neutron transmission of H_2O (=0.46 for λ = 10 Å and 1-mm path length). The term

$$\left[\frac{\sum b}{M_r} - \rho_s\left(\frac{V}{M_r}\right)\right]$$

is the contrast term defined by the sample and solvent chemistry, where $\sum b/M_r$ = scattering per unit molecular weight in the particle, $\sum b$ = sum of the scattering lengths (scattering power) of the constituent atoms, ρ_s = scattering density of the solvent, and V = particle volume; $V/M_r = \bar{v}/N_A$, where $\bar{v}$ = partial specific volume. For calculation of μ, the following values were used [computed from the tables in Jacrot (1976)]: for recA, $\sum b/M_r = 2.23 \times 10^{-14}$ cm/dalton and $\bar{v} = 0.74$ cm^3/g; for ds H-DNA, $\sum b/M_r = 3.18 \times 10^{-14}$ cm/dalton and $\bar{v} = 0.55$ cm^3/g; for solvent water, $\rho_s = -0.56 \times 10^{-14}$ cm/Å^3; and for solvent glycerol, $\rho_s = 0.61 \times 10^{-14}$ cm/Å^3.

$[I(Q)Q]_{Q\to 0}$ also allows the determination of the experimental matchpoint in contrast variation from plots of $[[I(Q)Q]_{Q\to 0}]^{1/2}$ versus D_2O volume fraction.

Contrast Variation. Contrast is defined as the difference between the scattering density of the macromolecule (ρ) and that of the solvent (ρ_s). It can be varied by changing the scattering density of the solvent in varying the D_2O/H_2O ratio. The *matchpoint* is that D_2O volume fraction where the contrast is 0. $\Delta\rho$, the value that is accessible to measurement, is the difference between the scattering density of the solute at the matchpoint and that of the solvent at any given D_2O/H_2O volume fraction. A plot of the square of the measured R_c versus the inverse of $\Delta\rho$ (Stuhrmann plot) reveals the relative positions of two components in a complex (Ibel & Stuhrmann, 1975) and will be discussed under Results.

Model Culculations. For a rod consisting of two concentric cylinders of radii R_1 and R_2, the cross-sectional radius of gyration is expressed as

$$R_c^2 = [f_1 R_1^2 + f_2(R_2^2 + R_1^2)]/2$$

where f_1 and f_2 are the relative contributions of the two cylinders to the total scattering.

To calculate the scattering of a model consisting of a protein shell surrounding a DNA core (Figure 2), we (i) calculated the excess scattering density (the contrast as defined above) of each component from its chemical composition (Jacrot, 1976), an assumed labile D–H exchange of 80% for the protein and 100% for DNA, and its molecular volume, to obtain $\rho - \rho_s$ as a function of the D_2O volume fraction X (see Table I); (ii) multiplied by the dry volume of that component in the shell to obtain the excess scattering of each shell; and (iii) hence obtained their relative contribution to the total scattering, f_1 and f_2.

Matchpoint. The matchpoint is that solvent composition for which the contrast is zero. This is calculated from the chemical formulas of the constituents, the only unknowns being the partial specific volume and the degree of exchange of labile hydrogens. It is normally assumed that 80% of labile protons are exchanged in proteins [see discussion in Perkins (1986)] and 100% in nucleic acids. This leads to calculated matchpoints of 41.9% D_2O for the complex with D-DNA and 39.0% for the homopolymers. The discrepancy between these values and the experimentally determined matchpoints (39.2% D_2O for the complex, 38.0% for the homopolymers) may reflect a reduced accessibility of solvent due to the polymerized state of the protein. A difference of 2–3% in the matchpoint has essentially no effect on the Stuhrmann plot. In the following we used the experimental matchpoint for both the experimental and theoretical calculations.

Table I: Scattering Densities of the Components of Solutions of recA Complexes[a]

	ρ in H_2O	ρ in D_2O	$\rho(X)$	$\rho(X) - \rho_s(X)$
water	−0.56	6.41	$-0.56 + 6.97X$	
glycerol	0.61			
5% glycerol buffer			$-0.50 + 6.97X = \rho_s(X)$[b]	
recA protein	1.82	3.04	$1.82 + 1.22X$	$2.32 - 5.75X$
recA$^{80\% exch}$	1.82	2.80	$1.82 + 1.02X$	$2.32 - 5.95X$
H-DNA	3.49	4.23	$3.49 + 0.74X$	$3.99 - 6.23X$
D-DNA	6.91	7.65	$6.91 + 0.74X$	$7.41 - 6.23X$

[a] ρ = scattering density = $\sum b/V$ ($\times 10^{-14}$ cm/Å^3). $\rho(X)$ = scattering density as a function of the D_2O volume fraction X. $\rho(X) - \rho_s(X)$ = excess scattering density of the solute with respect to the solvent (contrast). [b] All the contrast variation experiments were performed in 5% glycerol.

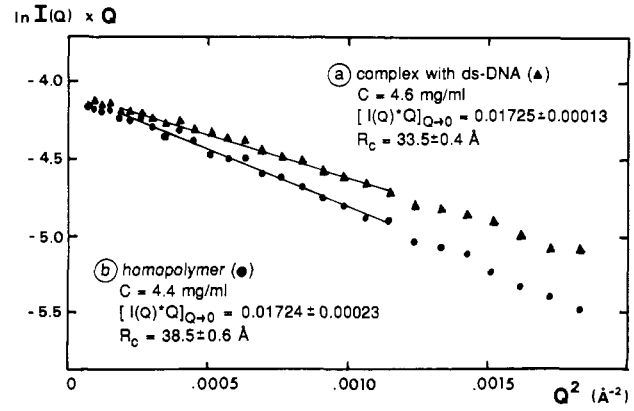

FIGURE 1: Cross-sectional Guinier plots. Typical example of a plot for the complex with ds DNA (linearized plasmid pUC8) (a), superimposed with a plot of the homopolymer (b). The values of R_c and $[I(Q)Q]_{Q\to 0}$ obtained in these two experiments are shown.

Results

Structure of Filamentous recA Complexes from Guinier Analysis

Plots of ln $I(Q)Q$ versus Q^2 yield the following results (Figure 1): *Complexes of recA with ds DNA* have a cross-sectional radius of gyration R_c = 33.3 ± 1.5 Å (nine determinations) and a mass per unit length of 2.20 ± 0.12 kDa/Å (n = 9). *Rods of recA homopolymer* have a cross-sectional radius of gyration R_c = 39.7 ± 1.7 Å (n = 10) and a mass per unit length of 2.36 ± 0.17 kDa/Å (n = 10). The values for the homopolymer vary strongly between experiments (extreme R_c of 36.9 and 41.6 Å). Electron microscopy revealed particles of 100–200-Å diameter contaminating samples of low R_c (the rods were indeed lost altogether in "homopolymer" samples of R_c = 35 Å). This observation of a degradation product allows us to interpret the scatter of the data as a consequence of lower stability of the homopolymer.

The mass per length of the complex with DNA has previously been measured by scanning transmission electron microscopy of unstained specimen to be 6.4 ± 0.6 recA units/100 Å (DiCapua et al., 1982) and is predicted to be 6.5 recA/100 Å from models derived from biochemical data and electron microscopy (Figure 2; Stasiak et al., 1983) as well as image reconstruction of negatively stained specimen (Egelman &

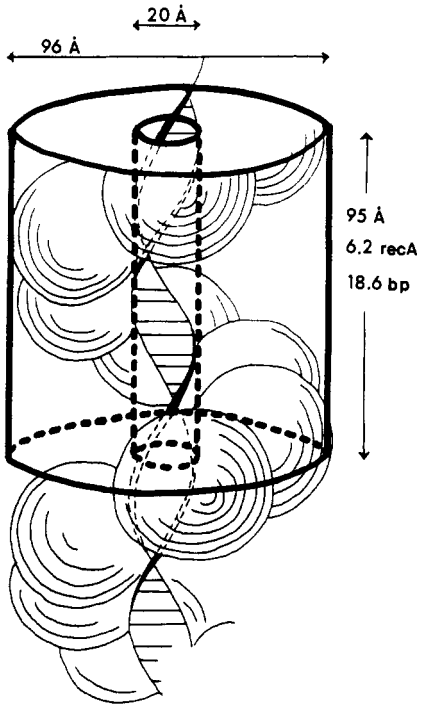

FIGURE 2: The complex of recA protein with ds DNA and the cylindrical model used for the calculation of R_c. A 95-Å length element is composed of a central cylinder containing 18.6 bp of DNA and an outer cylindrical shell containing 6.2 recA protein molecules. The details in the drawing have been obtained by electron microscopy and are shown as a reference. The exact number of subunits in the shell has little influence on the calculation.

Stasiak, 1986). The value obtained here by solution scattering corresponds to 5.5 ± 0.3 recA/100 Å (recA has M_r = 37.8K), that is, a value roughly compatible but 18% too low. We believe that the result does not contradict the former data for the following reasons: (i) The average of nine experiments (2.20 kDa/Å) has a large standard deviation (±0.12 kDa/Å) as compared to the error due to counting statistics and simple error propagation in a single determination (2.23 ± 0.04 kDa/Å in the typical plot of Figure 1). This variation is due in part to the choice of the fitting range along the linear plot: the Guinier approximation is strictly valid for infinitely long rigid rods, and our samples (in particular the homopolymers) are not such particles. Although the nonlinearity is not apparent, we have observed that the same data can be fitted with different values of R_c, beyond the statistical error; however, we were not able to pinpoint a consistent behavior in this fitting—as would arise if all samples were contaminated with the same kind of interfering particles, e.g., aggregates or, indeed, monomers. (ii) Interfering particles of heterogeneous size would scatter in a broad range of Q; they may contribute to some extent to the scattering in the range considered and ought to be subtracted as background. However, this is not feasible as we were not able to define them. (iii) These same particles may also contribute to a wrong estimate of the concentration of the particle of interest in the sample. Its value is critical for the calculation of the mass per length. This concentration is very likely to be overestimated, as the determination of concentration by absorbance includes impurites (e.g., heterogeneous polypeptide contaminants; see Materials and Methods).

Models of Filamentous recA Complexes

(*1*) *Mass per Unit Length.* The mass per unit length of the complex corresponding to 5.5 recA units per turn of a 95-Å helix is only roughly in agreement with the value determined from electron microscopy. This is probably due to the uncertainties in concentration described above; hence we see no contradiction to the model deduced previously (Figure 2).

The value for the homopolymer has never been estimated previously. We find a value of 6.2 recA/100 Å. This value is subject to similar concentration errors as for the complex and is therefore likely to be an underestimate. If it is scaled up in the same way as necessary to equate the SANS and EM results for the complex, we then obtain a value of 7.3 recA units/100 Å. Interestingly, it turns out to be the same value as the 6 recA per unit cell of 83 Å found in the $P6_1$ crystals of recA (McKay et al., 1980). The mass per length of the homopolymer is found to be about 13% greater than that of the complex. This is not surprising in view of the fact that electron microscopy as well as the R_c in solution suggest a different organization of the two structures.

(*2*) *Diameter of the Filaments.* A diameter of 100–110 Å was determined for the complexes with ds DNA by electron microscopy (DiCapua et al., 1982; Egelman & Stasiak, 1986). If this were a homogeneously filled cylinder, it would have an R_c of 35–39 Å. Clearly the situation is much more complex, since the cylinder is not filled homogeneously either chemically (DNA and protein) or spatially (open helix with a deep cleft). It is therefore tempting to compute an R_c from the known model, as sketched in Figure 2. A two-shell model with the DNA in a cylinder of 10-Å radius and the protein in a shell of 48-Å outer radius leads to 33.6 Å (see Materials and Methods), compatible with the experimental value of 33.3 ± 1.5 Å.

For the homopolymer, no detailed models have been proposed. Williams and Spengler (1985) estimate the width of unfixed rods to be about 110 Å. Our neutron scattering experiments reveal in addition a mass per length of 6–7 recA units/100 Å and a radius of gyration of about 40 Å. Were this a homogeneously filled cylinder, its actual radius would be 56 Å, and ~35% of its volume only would be protein (quite a loose packing). Approaching from another point of view, if we assume a packing similar to the one in the outer shell of the model of the complex (Figure 2), i.e., 44% of the shell is protein, then this would have as a consequence a central hollow of 18-Å radius, surrounded by a shell of 55-Å outer radius. In any case, the mere removal of the DNA from the model of Figure 2 (empty cylinder of 10-Å inner radius and 48-Å outer radius) would lead to an R_c of 34.7 Å, a number not compatible with the experimental value of 40 Å.

The level of accuracy of our measurements leaves open the precise number of recA subunits in the cylinder. This value however plays little role in the discussion of the contrast variation results.

Stuhrmann Plots

(*1*) *Calculated Stuhrmann Plots.* Model calculations were carried out to evaluate the magnitude of the variation of R_c that may be expected in contrast variation experiments. On the basis of the model of Figure 2 (as described under Materials and Methods), we calculated R_c as a function of the D_2O/H_2O content in the buffer, for complexes containing H-DNA and D-DNA, respectively. The result is displayed in the Stuhrmann plots in Figure 3A. This shows a linear dependence of R_c^2 on the inverse contrast, with higher values of R_c^2 in negative contrast (high D_2O content) than in positive contrast (H_2O). This behavior is typical for matter of higher scattering density being in the inner cylinder. The slope of the line is clearly steeper for D-DNA than H-DNA. The plot is drawn within the experimental limits of reasonably accurate measurements, i.e., up to 20% D_2O and above 60%. This

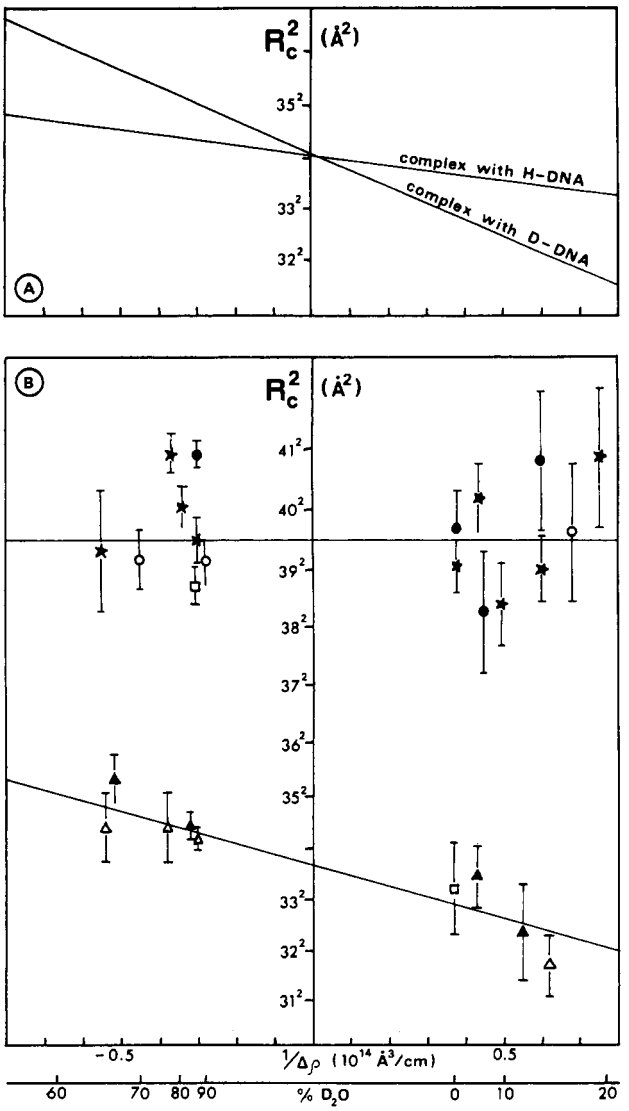

FIGURE 3: Stuhrmann plots, representing the variation of R_c with contrast, plotted as R_c^2 versus $1/\Delta\rho$. Some D_2O volume fractions are indicated for reference on the additional horizontal axis (only indicative because the reference matchpoints are slightly different for both samples). (A) Calculated from the model in Figure 2. (B) Stuhrmann plot obtained experimentally with complexes of recA with D-DNA (△, ▲) and from the homopolymer (○, ●, ★). The sets of symbols correspond to different experiments; the squares at 0% D_2O are the average from three experiments. The lines are the least-squares fits to the data points.

demonstrates that the maximal magnitude of the difference to be expected for H-DNA is 1.4 Å [from 33.3 Å (20% D_2O) to 34.7 Å (60% D_2O)] while it is 4.6 Å for D-DNA [from 31.6 Å (20%) to 36.2 (60%)].

Since the experimental uncertainty of a determination of R_c is in the order of 1 Å, we conclude that only an experiment with D-DNA is meaningful.

(*2*) *Experimental Stuhrmann Plots.* Careful measurements were made on complexes of recA protein with deuterated ds DNA as well as on homopolymers. R_c was determined from the slope of plots like those of Figure 1.

From these data, we obtained the Stuhrmann plot of Figure 3B. The least-squares fit through the data for the complex has a negative slope, demonstrating that the DNA is in the interior of the filament. The slope is very similar to the one obtained by calculation from the model of Figure 2, which confirms that the radial distribution of scattering density chosen in the model is a good representation of that in the actual complex. The exact slope of this line and its intersection with $1/\Delta\rho = 0$ are of course still imprecise due to the error in each data point, but this does not affect the qualitative result. As expected, the same experiment with H-DNA did not reveal a significant slope (not shown).

The R_c of the homopolymer did not vary systematically with contrast. The data points do however scatter considerably. We discussed in a previous section that the homopolymer was reproducibly less stable than the complex. We thus measured it in an additional set of experiments (stars in Figure 3B).

Discussion

Solution studies on macromolecular assemblies complement results obtained by electron microscopy. Here we have found a cross-sectional radius and a mass per length that support models obtained previously by electron microscopy. In addition, solution scattering with X-rays and neutrons reveals more about the inside of a structure than microscopy of stained specimens; while the latter rather describes the surface of the object, by solution scattering we obtain information about the internal distribution of mass.

This led to a first interesting finding, the significant change in conformation of recA upon binding of DNA; between the homopolymer rod and the complex filament, the cross-sectional radius of gyration decreases by 6.6 Å, which cannot be due to the mass of the DNA alone, as calculation predicts only a small change of about 1 Å (not shown). This finding may reflect the mechanism for activation of the protein from possibly a storage form into a conformation that will be active in the strand-transfer reaction and as an inducer of the SOS system (Roberts et al., 1978).

Neutron scattering has a further unique property in being able to distinguish molecules by their chemical composition, leading to the possibility of contrast variation in the analysis of multicomponent assemblies. This approach has been exploited successfully for a number of nucleo–protein complexes, including nucleosomes (Pardon et al., 1977), ribosomes [reviewed in Koch and Stuhrmann (1979)], filamentous complexes of gene V protein with DNA (Gray et al., 1982), and spherical viruses (Timmins, 1988). For these assemblies the relative weight of the nucleic acid component is much greater than it is in the case of the recA–DNA filaments, where the DNA represents only 4.7% by weight.

The negative slope of the Stuhrmann plot shows unambiguously that the DNA must be close to the center of the recA–DNA filament. We can thus exclude any kind of "side-by-side" association of the macromolecules. A comparison of the experimental and calculated Stuhrmann plots shows that a protein shell of 96-Å diameter surrounding a DNA core of 20-Å diameter fits the data quite well. The diameter of 96 Å is close to that observed by scanning transmission electron microscopy (DiCapua et al., 1982) and in negative stain (Egelman & Stasiak, 1986). The experimental Stuhrmann plot is rather less steep than that calculated from the model; this could be the result of some interpenetration of the protein and DNA shells, including a possible coiling of the DNA path at about 9-Å radius as discussed in Egelman and Stasiak (1986). It could however also be due to incomplete exchange of the labile protons of the protein, due to its highly polymerized state, which may reduce solvent accessibility. Further, we have assumed that the 5% glycerol is homogeneously distributed in the solvent and not excluded from some regions close to the protein. Such an effect has been observed for globular proteins (Lehmann & Zaccai, 1984) and is discussed in detail for the complex of DNA with RNA polymerase (Heumann et al., 1988), however, in solutions of considerably higher glycerol content. Our model

calculations were based on a 100% deuterated DNA whereas the experiment used DNA of unknown degree of deuteration, estimated to be at least 80% as it was produced in 100% D_2O with deuterated succinate as a carbon source; incomplete deuteration of the DNA would also lead to a flatter Stuhrmann plot. The inherent error of the experimental data does not allow conclusions at a higher level of precision.

The results outlined above constitute the first experimental evidence that the DNA is localized close to the center of the recA–DNA filaments as has been suggested earlier for the theoretical reason that the chemical bonds of the DNA could not be extended such as to be wrapped around the outside of the protein. Our results add support to the hypothesis that for the strand exchange reaction between two DNA molecules, the second partner must find its way *into* the complex, presumably through the deep cleft of the helical complex detected by electron microscopy (DiCapua et al., 1982; Howard-Flanders et al., 1984).

ACKNOWLEDGMENTS

We thank M. T. Dauvergne and R. Leberman for the production of deuterated *E. coli*.

Registry No. Neutron, 12586-31-1.

REFERENCES

Bryant, F. R., Taylor, A. R., & Lehman, I. R. (1985) *J. Biol. Chem. 260*, 1196–1202.

Cassuto, E., & Howard-Flanders, P. (1986) *Nucleic Acids Res. 14*, 1149–1157.

Craig, N. L., & Roberts, J. W. (1981) *J. Biol. Chem. 256*, 8039–8044.

DiCapua, E., & Koller, Th. (1987) in *Nucleic Acids and Molecular Biology*, Vol. 1, pp 175–185, Springer, Berlin.

DiCapua, E., & Müller, B. (1987) *EMBO J. 6*,2493–2498.

DiCapua, E., Engel, A., Stasiak, A., & Koller, Th. (1982) *J. Mol. Biol. 157*, 87–103.

Dombroski, D. F., Scraba, D. G., Bradley, R. D., & Morgan, A. R. (1983) *Nucleic Acids Res. 11*, 7487–7504.

Egelman, E., & Stasiak, A. (1986) *J. Mol. Biol. 191*, 677–697.

Flory, J., Tsang, S. S., & Muniyappa, K. (1984) *Proc. Natl. Acad. Sci. U.S.A. 81*, 7026–7030.

Ghosh (1981) ILL Internal Report 81GH29T.

Gray, D. M., Gray, C. W., & Carlson, R. D. (1982) *Biochemistry 21*, 2702–2713.

Heumann, H., Lederer, H. Baer, G., May, R. P., Kjems, J. K., & Crespi, H. L. (1988) *J. Mol. Biol. 201*, 115–125.

Howard-Flanders, P., West, S. C., & Stasiak, A. (1984) *Nature 309*, 215–220.

Ibel, K. (1976) *J. Appl. Crystallogr. 9*, 296–309.

Ibel, K., & Stuhrmann, H. B. (1975) *J. Mol. Biol. 93*, 255–265.

Jacrot, B. (1976) *Rep. Prog. Phys. 39*, 911–953.

Jacrot, B., & Zaccai, G. (1981) *Biopolymers 20*, 2413–2426.

Kalbitzer, H. R., Leberman, R., & Wittinghofer, A. (1985) *Febs. Lett. 180*, 40–42.

Koch, M. H. J., & Stuhrmann, H. B. (1979) *Methods Enzymol. 59*, 670–706.

Koller, Th., DiCapua, E., & Stasiak, A. (1983) in *Mechanisms of DNA Replication and Recombination* (Cozzarelli, N. R., Ed.) pp 723–730, Liss, New York.

Leahy, M. C., & Radding, C. M. (1986) *J. Biol. Chem. 261*, 6954–6960.

Lehmann, M. S., & Zaccai, G. (1984) *Biochemistry 23*, 1939–1942.

Pardon, J. F., Cotter, R. I., Lilley, D. M. J., Worcester, D. L., Campbell, A. M., Woolley, J. C., & Richards, B. M. (1977) *Cold Spring Harbor Symp. Quant. Biol. 42*, 11–22.

Perkins, S. J. (1986) *Eur. J. Biochem. 157*, 169–180.

Roberts, J. W., Roberts, C. W., & Craig, N. L. (1978) *Proc. Natl. Acad. Sci. U.S.A. 75*, 4714–4718.

Stasiak, A., & DiCapua, E. (1982) *Native 299*, 185–186.

Stasiak, A., DiCapua, E., & Koller, Th. (1981) *J. Mol. Biol. 151*, 557–564.

Stasiak, A., DiCapua, E., & Koller, Th. (1983) *Cold Spring Harbor Symp. Quant. Biol. 47*, 811–819.

Timmins, P. A. (1988) *Makromol. Chem., Makromol. Symp. 15*, 311–321.

Timmins, P. A., & Zaccai, G. (1988) *Eur. Biophys. J. 15*, 257–268.

Torbet, J., Gray, D. M., Gray, C. W., Marvin, D. A., & Siegrist, H. (1981) *J. Mol. Biol. 146*, 305–320.

Tsang, S. S., Muniyappa, K., Azhderian, E., Gonda, D. K., Radding, C. M., Flory, J., & Chase, J. (1985) *J. Mol. Biol. 185*, 295–309.

Weinstock, G. M., McEntee, K., & Lehmann, I. R. (1979) *Proc. Natl. Acad. Sci. U.S.A. 76*, 1638–1642.

West, S. C., Cassuto, E., Mursalim, J., & Howard-Flanders, P. (1980) *Proc. Natl. Acad. Sci. U.S.A. 77*, 2569–2573.

West, S. C., Cassuto, E., & Howard-Flanders, P. (1981) *Proc. Natl. Acad. Sci. U.S.A. 78*, 6149–6153.

Williams, R. C., & Spengler, S. J. (1986) *J. Mol. Biol. 187*, 109–118.